

Title	Experimental investigation of a bistable system in the presence of noise and delay
Authors	Houlihan, John;Goulding, David;Busch, Thomas;Masoller, C;Huyet, Guillaume
Publication date	2004
Original Citation	Houlihan, J., Goulding, D., Busch, T., Masoller, C. and Huyet, G. (2004) 'Experimental investigation of a bistable system in the presence of noise and delay', Physical Review Letters, 92(5), 050601 (4pp). doi: 10.1103/PhysRevLett.92.050601
Type of publication	Article (peer-reviewed)
Link to publisher's version	<a href="https://journals.aps.org/prl/abstract/10.1103/PhysRevLett.92.050601">https://journals.aps.org/prl/abstract/10.1103/PhysRevLett.92.050601</a> - 10.1103/PhysRevLett.92.050601
Rights	© 2004, American Physical Society
Download date	2023-05-06 01:15:32
Item downloaded from	<a href="http://hdl.handle.net/10468/4655">http://hdl.handle.net/10468/4655</a>

# Experimental Investigation of a Bistable System in the Presence of Noise and Delay

J. Houlihan,<sup>1</sup> D. Goulding,<sup>1</sup> Th. Busch,<sup>1</sup> C. Masoller,<sup>2</sup> and G. Huyet<sup>1</sup>

<sup>1</sup>*Physics Department, National University of Ireland, University College Cork, Cork, Ireland*

<sup>2</sup>*Instituto de Física, Facultad de Ciencias, Universidad de la República, Igua 4225, Montevideo 11400, Uruguay*

(Received 13 May 2003; published 6 February 2004)

We experimentally analyze the behavior of a non-Markovian bistable system with noise, using a vertical cavity surface emitting laser with time-delayed optoelectronic feedback. The effects of the delayed feedback are observed in the probability distribution of the residence times of the two orthogonal polarization states, and in the polarization-resolved power spectrum. They agree well with recent theoretical predictions based on a two-state model with transition rates depending on an earlier state of the system. We also observe experimentally and explain theoretically that the residence time probability distribution deviates from exponential decay for residence times close to (and smaller than) the delay time.

DOI: 10.1103/PhysRevLett.92.050601

PACS numbers: 05.40.Ca, 05.45.-a, 42.65.Pc, 42.65.Sf

Since the pioneering work of Kramers [1] on thermally activated barrier crossing, the properties of bistable systems under the influence of noise have become a subject with relevance in a wide range of fields such as physics, chemistry, and biology [2,3]; stochastic resonance being one of the areas which has received considerable attention [4]. Various mathematical tools have been developed to study noise-activated escape processes, mostly using the Markovian assumption that the system evolves slowly compared to the time scale of the correlations of the random forces [5,6]. Recently, non-Markovian stochastic processes have also been the subject of increased interest [7–13].

The essential features of Kramers escape problem can be captured by considering a stochastic variable  $x(t)$  that switches between two metastable states  $x_1$  and  $x_2$  at random times  $t_i$ . If the residence time intervals  $T_i = t_i - t_{i-1}$  are independently distributed, the dynamics can be reduced to a Markovian process and the residence time distribution (RTD) has an exponential shape [1]

$$P_{1,2}(T) = \frac{1}{T_{1,2}^K} \exp\left[-\frac{T}{T_{1,2}^K}\right]. \quad (1)$$

This relation is usually referred to as Kramers' law and the mean residence times,  $T_{1,2}^K$  are the Kramers' times for states  $x_1$  and  $x_2$ .

In certain systems, the stochastic process  $x(t)$  can exhibit strong temporal long range correlations and the RTDs are found to be nonexponential. A special case of such a non-Markovian process is time-delayed feedback, where the current state of the system depends on an earlier state at fixed time. An equation of motion for such time-delayed dynamical systems can be written as

$$\dot{x}(t) = -\frac{\partial}{\partial x} U[x(t), x(t-\tau)] + \sqrt{D}\zeta(t), \quad (2)$$

where  $\zeta(t)$  describes a random process with a white Gaussian noise profile and intensity  $D$ . The delay interval

is fixed as  $\tau$  and an example of a delayed, symmetric, and bistable potential is given by

$$U = -x^2(t) + x^4(t) - \epsilon x(t)x(t-\tau), \quad (3)$$

where  $\epsilon$  is the amplitude of the feedback signal. Such stochastic delay systems with additive noise have recently been examined using Fokker-Planck equations [7,8,10,12]. When the system is linear or when the delay time is small compared to the Kramers times, exact solutions of the Fokker-Planck equation can be derived. To study nonlinear delayed systems with an arbitrary delay time Tsimring and Pikovsky [9] have considered a two-state system,  $s(t) = \pm 1$ , where the transition rate,  $p(t)$ , can take one of two values depending on the value of the variable at a delayed arbitrary time  $s(t-\tau)$

$$p(t) = p_1 \quad \text{if } s(t-\tau) = s(t), \quad (4)$$

$$p(t) = p_2 \quad \text{if } s(t-\tau) = -s(t). \quad (5)$$

The autocorrelation function and the power spectrum were derived for this model and the latter was found to exhibit peaks at frequencies related to the delay time. For  $\epsilon > 0$ , the peaks are located near frequencies  $\nu_n \sim n/\tau$ , while for  $\epsilon < 0$  the peaks are located near frequencies  $\nu_n \sim 1/2\tau + n/\tau$ ,  $n = 0, 1, 2, \dots$ . The amplitude of the main peak was found to have a maximum at a certain noise level, thus demonstrating coherence resonance.

The RTD for the two-state model was calculated in [11]. While in the absence of feedback it shows a simple exponential decay (1), pronounced discontinuities at  $T = \tau$  were predicted when introducing the delay term. Additionally, it was found that for a positive or negative feedback amplitude the probabilities for residence times smaller than the delay time are enhanced or decreased, respectively.

Here, we present a detailed experimental study of a bistable system with noise and time-delayed feedback. We first show that the two polarization states of a vertical

cavity surface emitting laser (VCSEL) operating in a bistable region closely follow the model used in [9,11]. We then measure the RTDs and confirm the appearance of a discontinuity at  $T = \tau$ . We also find experimentally a deviation from exponential behavior for residence times close to (and smaller than)  $\tau$ , and explain this within the two-state model. Finally, we measure the power spectrum and find resonances as predicted by the two-state model.

The output of a VCSEL is usually linearly polarized along one of the two orthogonal directions associated with crystalline or stress orientations (referred to as the  $x$  and  $y$  axes). At threshold one linear polarization dominates, but as the injection current is increased, devices commonly exhibit a switch to the orthogonal polarization state. Around this switching point, a range of injection currents can be found where the laser spontaneously changes between the two polarization states [14].

Previous experimental investigations of VCSELs have shown that the polarization switching follows Kramers' law both in the case where the noise is supplied to the laser on the bias current [15] and in the case where the noise is the intrinsic, spontaneous emission noise of the laser [14]. Using a Langevin formalism for the temporal evolution of the polarization state, these observations can be explained employing a phenomenological double-well potential,  $V(x)$ , for injection currents within the bistable region. Its shape can be constructed by fitting the experimental histograms of the polarization intensity for different values of the injection current [16]. In addition, stochastic resonance [4] was demonstrated when a weak periodic modulation was superimposed on the dc injection current [15].

The experimental setup is shown in Fig. 1(a). Light is emitted from a VCSEL which is temperature controlled to within 10 mK at 850 nm and coupled into an avalanche

photodiode after passing through a polarizer. By choosing the orientation of the polarizer, the  $x$  or the  $y$  polarization can be selected for reinjection into the laser. A coaxial cable is used to delay the electronic signal before it is added to the dc laser bias current. The electronic feedback loop has an effective low frequency cutoff of 1 kHz and a bandwidth limited to a few hundred MHz. The subsequent dynamics, with and without feedback, always lies well within this bandwidth and the main effect of the low frequency cutoff is to remove the dc component of the delayed signal.

After passing through the polarizer  $P$ , the light intensity can assume the two values:  $I = 0$  and  $I = I_0$ . Accordingly, after traveling through the delay line, the total current injected into the VCSEL is  $J = J_{dc} - J_0$  if  $I(t - \tau) = 0$  or  $J = J_{dc} + J_0$  if  $I(t - \tau) = I_0$ . Here  $J_0$  scales with the strength of the feedback and is determined by measuring the voltage at the combination electronics (minicircuits ZFBT-6GW). Typical values for our experiment are  $J_{dc} = 2$  mA and  $J_0 = 0.09$  mA. A digital oscilloscope (LeCroy WM8600) is used to acquire data from the diagnostic arm of the experiment (detector rise time is 1 ns) where a second polarizer ( $P_d$ ) allows for polarization selective measurement.

The polarization-resolved output power versus injection current of our device in the absence of feedback is shown in Fig. 1(b). The laser emits in either the  $x$  or  $y$  polarization with a small region ( $1.9$  mA  $< I < 2.1$  mA) of the injection current where spontaneous polarization switching occurs. To show that our device indeed behaves as a two-state system with noise governed dynamics, we first reproduce the Kramers' relation of Eq. (1) (see thin lines in Figs. 2 and 3). The Kramers decay times  $T_x^K$  and  $T_y^K$  are usually different due to anisotropies of the two polarization states, and can be varied by changing the injection current. At the high current side of the bistability region [see Fig. 1(b)] the  $y$  ( $x$ ) polarization state is more (less) favorable and thus has a higher (lower)

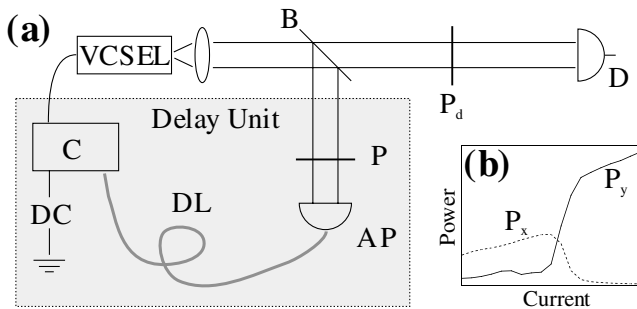


FIG. 1. (a) Schematic of the experimental setup: Light from the VCSEL is split at a beam splitter ( $B$ ) into a delay arm and a detection arm, both including a polarizer ( $P$ ,  $P_d$ ). The avalanche photodiode ( $AP$ ) at the end of the delay arm couples to the delay line ( $DL$ ). At its end, the delayed current is added to the dc bias current ( $DC$ ). Finally, the optically isolated signal is detected at  $D$ . (b) Polarization resolved power-current characteristic of the VCSEL in the bistability region.  $P_x$  and  $P_y$  denote the polarizations along the  $x$  and  $y$  directions, respectively.

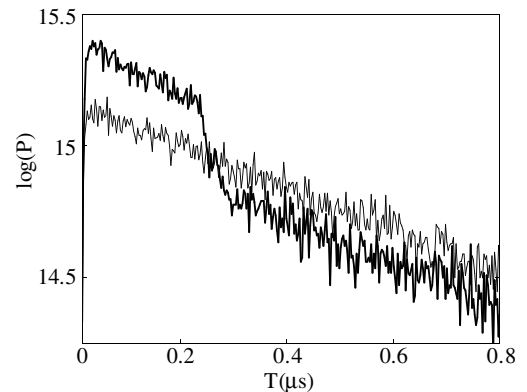


FIG. 2. RTD for the  $x$  state without feedback (thin line) and with feedback proportional to the delayed intensity of the  $y$ -polarized state (bold line).

Kramers residence time. The opposite situation occurs on the low current side. In the following, the value of the dc injection current is chosen in order to have similar Kramers times for each of the two polarization states.

In Fig. 2, the RTD of the  $x$ -polarized state is shown for the case where the delay line polarizer selects the  $y$  polarization (bold line). Apart from a dramatic steplike behavior around  $T \sim \tau$ , one can clearly see that residence times shorter than the delay time become more probable while residence times longer become less probable. The opposite is the case when the delay line polarizer selects the  $x$  polarization (see Fig. 3), where residence times shorter than the delay time become less probable while residence times longer than the delay time become more probable.

The results of Figs. 2 and 3 are qualitatively consistent with the numerical predictions in [11] for positive and negative feedback coefficients, respectively, and their interpretation for the case of the VCSEL is straightforward. Let us, with no loss of generality, consider the situation where the laser has emitted  $y$ -polarized light for  $t < 0$  and a polarization switch has happened at  $t = 0$ . If the delay line polarizer is set in the  $y$  direction, the total injection current is given by

$$J(t) = J_{dc} + J_0 \quad \text{for } 0 < t < \tau, \quad (6)$$

$$J(t) = J_{dc} - J_0 \quad \text{for } t > \tau. \quad (7)$$

Thus, for  $0 < t < \tau$  the current is increased ( $J > J_{dc}$ ) and one can see from Fig. 1(b) that the  $x$  state becomes less stable than in the absence of the feedback ( $J = J_{dc}$ ) and the probability of switching into the  $y$  state increases. For  $t > \tau$ , the current is reduced ( $J < J_{dc}$ ) and the  $x$  state is more stable and, consequently, the probability of switching decreases. Therefore the RTD increases for  $T < \tau$  and decreases for intervals larger than the delay time (see Fig. 2). Using an  $x$  polarizer in the delay arm instead the effect is exactly inverted, as can be seen in Fig. 3. The situation for  $y$ -polarized light can be straightforwardly explained in an analogous way.

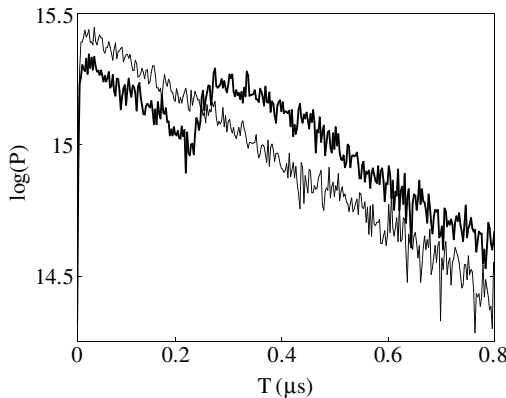


FIG. 3. As Fig. 2 but with the delayed intensity of the  $x$ -polarized state.

It is interesting to study the RTD in more detail. Even though the strict exponential behavior is already broken by the discontinuity at  $T = \tau$ , it still follows a piecewise exponential behavior for  $T \ll \tau$  and for  $T > \tau$ . Remarkably, one can observe that the distribution deviates from exponential decay for residence times  $T$  smaller and close to  $\tau$  as shown in Fig. 4. In fact, depending on the sign of feedback, the decay rate increases or decreases relative to its value at  $T \ll \tau$ . We have performed numerical simulations of the two-state model in the same regime and obtained similar statistics (solid line in Fig. 4). While one can immediately see [11] that the decay rate of the probability function for  $T \rightarrow \tau$  (while  $T < \tau$ ) approaches  $p_2$  (and is  $p_1$  for  $T > \tau$ ), the value of the decay rate for  $T \ll \tau$  is not obvious and we find it to be  $p(T < \tau - T^K) = \sqrt{p_1 p_2}$  as shown by the dashed line in Fig. 4, where  $T^K$  is the mean residence time.

To calculate the RTD in this limit, we can first calculate the switching rate averaged over many trajectories. It can be written (as a function of the normalized time  $\theta = t/\tau$ ) as

$$\langle p(\theta) \rangle = \frac{p_1 + p_2}{2} + \frac{p_1 - p_2}{2} \langle s(\theta) s(\theta - 1) \rangle. \quad (8)$$

Here, the quantity  $C_s(1) = \langle s(\theta) s(\theta - 1) \rangle$  is the autocorrelation of the variable  $s(\theta)$  under the constraint that a switch at  $\theta = 0$  has occurred. This differs from the autocorrelation function,  $C$ , calculated in Ref. [9], where no such constraint was imposed. In the limit where  $\theta^K = T^K/\tau \rightarrow 0$ , i.e., the limit where the mean switching time goes to zero, the constraint of Ref. [9] is equivalent to the existence of a switch when  $\theta = 0$ . Thus, when  $\theta < \tau - \theta^K$ ,

$$\lim_{\theta^K \rightarrow 0} C_s(1) = \lim_{\theta^K \rightarrow 0} C(1) = \frac{\sqrt{p_2} - \sqrt{p_1}}{\sqrt{p_1} + \sqrt{p_2}}. \quad (9)$$

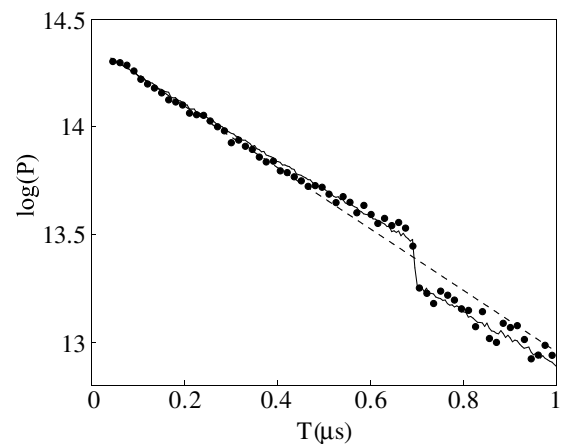


FIG. 4. Residence time distributions obtained from experiment (dots) and numerical simulation of two-state model (solid line). Dashed line corresponds to an exponential decay of slope  $\sqrt{p_1 p_2}$ . The two-state model was simulated for  $p_1 = 1.5 \mu s^{-1}$  and  $p_2 = 1.24 \mu s^{-1}$ . The delay in both cases was  $\tau = 0.7 \mu s$ .

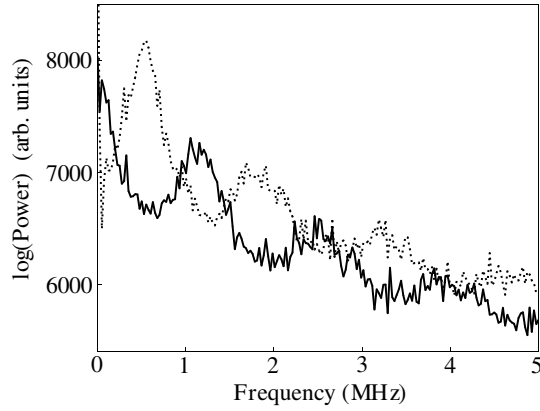


FIG. 5. Power spectra corresponding to the situations depicted on Fig. 2 (solid line) and Fig. 3 (dashed line).

From this, one straightforwardly finds  $p(T \ll \tau) = \sqrt{p_1 p_2}$ . As  $\theta$  approaches 1,  $C_s(1) \rightarrow -1$  and  $p(\theta) \rightarrow p_2$ . Thus,  $p(t)$  can vary strongly in the time interval  $[\tau - T^K, \tau]$ . It is interesting to note that this remarkable result shows that, even in the limit of  $T^K/\tau \rightarrow 0$ , the system differs from one with a random switching rate, varying between  $p_1$  and  $p_2$ , where one would expect  $p = (p_1 + p_2)/2$ . This is due to the presence of long range correlations in the time-delayed system.

Finally, in Fig. 5 we present the effect of feedback on the polarization-resolved power spectrum, for the  $x$ -polarization state. The solid line (dashed line) shows the spectrum when feedback is proportional to the delayed intensity of the  $y$  state ( $x$  state). In both cases, peaks associated with multiples of the delay time appear. In the first case, maxima are observed at  $\nu_n = n/\tau$  and minima at  $(2n + 1)/2\tau$ . When the delay line polarizer is rotated by  $90^\circ$ , the frequencies  $\nu_n = n/\tau$  correspond to minima while  $\nu_n = (2n + 1)/2\tau$  correspond to maxima, which is in excellent agreement with the analytic predictions of [9].

In conclusion, the analysis of the polarization switching phenomenon of a bistable VCSEL with optoelectronic feedback provides interesting insights on the dynamics of bistable systems under the influence of noise and delayed feedback. We have presented the first experimental investigation of the two-state model with transition rates depending on the past as theoretically studied in [9,11], and we have observed many features predicted for this model. Additionally, we have found experimentally a

nonexponential decay of the RTD for residence times close to and smaller than the delay time, and explained it theoretically within the two-state model.

The authors acknowledge I. Kardosh, V. Voignier, and J. O'Callaghan at the Department of Optoelectronics, University of Ulm, Germany, for the VCSEL samples, and R. Gillen and J. Sheehan for technical assistance. This work was supported by Science Foundation Ireland under Contract No. sfi/01/fi/co, by the TMR program of the commission of the European Union through the VISTA network, and the Irish Research Council for Science, Engineering and Technology.

- 
- [1] H. A. Kramers, *Physica* (Amsterdam) **7**, 284 (1940).
  - [2] P. Hänggi, P. Talkner, and M. Borkovec, *Rev. Mod. Phys.* **62**, 251 (1990).
  - [3] J. Dunkel, W. Ebeling, L. Schimansky-Geier, and P. Hänggi, *Phys. Rev. E* **67**, 061118 (2003).
  - [4] L. Gammaitoni, P. Hänggi, P. Jung, and F. Marchesoni, *Rev. Mod. Phys.* **70**, 223 (1998).
  - [5] C.W. Gardiner, *Handbook of Stochastic Methods: For Physics, Chemistry and the Natural Sciences* (Springer-Verlag, Berlin, 2002).
  - [6] M. San Miguel and R. Toral, *Instabilities and Nonequilibrium Structures VI*, edited by E. Tirapegui, J. Martínez, and R. Tiemann (Kluwer Academic Publishers, Dordrecht, 2000), p. 35–130.
  - [7] S. Guillouzie, I.L. Heureux, and A. Longtin, *Phys. Rev. E* **59**, 3970 (1999).
  - [8] S. Guillouzie, I.L. Heureux, and A. Longtin, *Phys. Rev. E* **61**, 4906 (2000).
  - [9] L. S. Tsimring and A. Pikovsky, *Phys. Rev. Lett.* **87**, 250602 (2001).
  - [10] T.D. Frank and P.J. Beek, *Phys. Rev. E* **64**, 021917 (2001).
  - [11] C. Masoller, *Phys. Rev. Lett.* **90**, 020601 (2003).
  - [12] T.D. Frank, P.J. Beek, and R. Friedrich, *Phys. Rev. E* **68**, 021912 (2003).
  - [13] I. Goychuk and P. Hänggi, *Phys. Rev. Lett.* **91**, 070601 (2003).
  - [14] M. B. Willemsen, M. U. F. Khalid, M. P. van Exter, and J. P. Woerdman, *Phys. Rev. Lett.* **82**, 4815 (1999).
  - [15] G. Giacomelli, F. Marin, and I. Rabbiosi, *Phys. Rev. Lett.* **82**, 675 (1999); S. Barbay, G. Giacomelli, and F. Marin, *Phys. Rev. E* **61**, 157 (2000).
  - [16] G. Giacomelli and F. Marin, *Quantum Semiclass. Opt.* **10**, 469 (1998).